Performance Bounds of MIMO Receivers in the Presence of Radio Frequency Interference

Aditya Chopra*, Kapil Gulati*, Brian L. Evans*, Keith R. Tinsley† and Chaitanya Sreerama†
* The University of Texas at Austin, Austin, Texas 78712
Email: {chopra, gulati, bevans}@ece.utexas.edu
†Intel Corporation, Santa Clara, CA 95054
Email: {keith.r.tinsley, chaitanya.sreerama}@intel.com

***Abstract*—Multi-input multi-output (MIMO) receivers have generally been designed and their communication performance analyzed under the assumption of additive Gaussian noise. Wireless transceivers, however, may also be affected by radio frequency interference (RFI) that is well modeled using non-Gaussian impulsive statistics. In this paper, we derive bounds on the communication performance for a two transmit, two receive antenna MIMO system in the presence of RFI. Our contributions include derivation of (1) channel capacity in the presence of RFI, (2) probability of symbol error for uncoded transmissions, and (3) Chernoff bound on the pairwise error probability and cutoff rate as a measure of the throughput performance for coded transmissions. Comparison with the communication performance bounds for receivers designed assuming additive Gaussian noise demonstrates degradation in communication performance in the presence of RFI.**

Index Terms: Electromagnetic radiative interference, MIMO systems, Communication system performance, Information rates, Error analysis, MAP estimation

I. Introduction

Wireless transceivers deployed on a computation platform (e.g. laptop computer) are greatly affected by the RFI generated by the clocks and buses on the platform itself [1]. RFI is a combination of independent radiation events and is well modeled using non-Gaussian impulsive statistics. In [2], it was demonstrated that conventional MIMO receivers designed assuming additive Gaussian noise, such as zero-forcing, maximum likelihood and space-time block coded systems, show degradation in communication performance in the presence of a mixture of Gaussian and impulsive noise.

Middleton Class A, B and C noise models [3] are perhaps the most common statistical-physical model for RFI. They have been shown to accurately model the non-linear phenomenon governing electromagnetic interference (EMI), and explicitly include a Gaussian component to account for receiver thermal noise [3]. In [4], performance bounds for symbol error rate optimal reception in the presence of Middleton Class A noise was studied for single antenna systems. In this paper, we extend this analysis to MIMO systems and derive the capacity and performance bounds in the presence of RFI.

Extending the Middleton models to multi-antenna systems is not straightforward. Many authors (e.g. [5], [6]) used a weighted sum of multivariate Gaussian densities to approximate the distribution of a Middleton Class A model. These models are not derived based on physical principles governing EMI. In [7], an extension to the Middleton Class A model was proposed for two antenna systems based on statistical physical principles. Hence, we restrict our attention to 2×2 MIMO systems using this bivariate Middleton Class A noise model which was demonstrated to accurately model RFI using measured RFI data acquired from a laptop embedded wireless transceiver in [8].

In this paper, we derive communication performance bounds for symbol error rate optimal reception are derived for a 2×2 MIMO system in the presence of bivariate Middleton Class A noise. The capacity of a memoryless channel in the presence of RFI is derived and compared to an additive Gaussian noise channel. The probability of error for uncoded transmission is derived using the symbol error rate optimal decision rule. For coded transmission, the Chernoff bound on the pairwise error probability and the corresponding cutoff rate analyzed under a random coding argument.

II. System Model

Consider a transmission system where both the transmitter and receiver are equipped with two antennas. The discrete-time baseband MIMO channel model can be expressed as

$$\mathbf{Y} = \sqrt{\frac{E_s}{2}}\mathbf{S} + \mathbf{N} \tag{1}$$

where $\mathbf{Y}$ is the $2 \times T$ matrix of received signals with T being the length of the transmitted data block, E_s is the total transmit energy, $\mathbf{S}$ is the $2 \times T$ transmitted data block and $\mathbf{N}$ is the $2 \times T$ matrix representing additive noise. The transmitted data block $\mathbf{S} = (\mathbf{s}_1, \mathbf{s}_2, \cdots, \mathbf{s}_T)$ is chosen from a codebook $\mathcal{S}$ with cardinality $|\mathcal{S}|$. The 2×1 code symbols $\mathbf{s}_t \in \mathcal{X}$, for $t \in [1, T]$, are derived from an arbitrary set of real or complex constellation points and chosen from a set of input alphabets $\mathcal{X}$ with cardinality $|\mathcal{X}|$.

Our additive noise model is the bivariate Middleton Class A model from [7]. The model represents narrowband RFI (i.e. noise spectrum bandwidth is less than the receiver bandwidth) and explicitly includes a Gaussian component. Since we assume that RFI is a sum of independent transmission events [3], the noise observations will be temporally independent and identically distributed (*i.i.d.*). Further, the in-phase and quadrature phase components of the noise ($\mathbf{N} = \mathbf{n}_I + j\mathbf{n}_Q$) are

This research was supported by Intel Corporation.

assumed to be *i.i.d.* such that the probability density function

$$f_{\mathbf{N}}(\mathbf{n}_I, \mathbf{n}_Q) = f_{\mathbf{n}_I}(n_{I,1}, n_{I,2}) \times f_{\mathbf{n}_Q}(n_{Q,1}, n_{Q,2}) \quad (2)$$

where $n_{I,k}$ and $n_{Q,k}$ denote the in-phase and quadrature phase noise signals at receiver antenna k, respectively, for $k = 0, 1$. The in-phase $(\mathbf{n}_I)$ and quadrature phase $(\mathbf{n}_Q)$ baseband noise components each have the joint spatial distribution [7]

$$f_{\mathbf{n}}(n_1, n_2) = \frac{e^{-A}}{2\pi|\mathbf{K}_0|^{\frac{1}{2}}} e^{\frac{-\mathbf{n}^T\mathbf{K}_0^{-1}\mathbf{n}}{2}} + \frac{\left(1-e^{-A}\right)}{2\pi|\mathbf{K}_1|^{\frac{1}{2}}} e^{\frac{-\mathbf{n}^T\mathbf{K}_1^{-1}\mathbf{n}}{2}} \quad (3)$$

where $|\cdot|$ denotes the determinant function and for $m = 0, 1$,

$$\mathbf{K}_m = \begin{bmatrix} (c_m)^2 & \kappa c_m \hat{c}_m \\ \kappa c_m \hat{c}_m & (\hat{c}_m)^2 \end{bmatrix} \quad (4)$$

$$(c_m)^2 = \frac{\frac{m}{A} + \Gamma_1}{1 + \Gamma_1}\ ,\ (\hat{c}_m)^2 = \frac{\frac{m}{A} + \Gamma_2}{1 + \Gamma_2}. \quad (5)$$

This model is uniquely determined by the following four parameters:

- A is the overlap index. It is the product of the average number of emission events impinging on the receiver per second and mean duration of a typical interfering source emission, $A \in [10^{-2}, 1]$ in general [9].
- Γ_1, Γ_2 are the ratios of the Gaussian to the non-Gaussian component intensity at each antenna, $\Gamma_1, \Gamma_2 \in [10^{-6}, 1]$ in general [9].
- κ is the correlation coefficient between the observations at the two antennas.

III. Capacity

Channel capacity is an upper bound on the rate at which information can be reliably transmitted over a channel, where reliable transmission means that the probability of error can be driven to zero by increasing the block length. Using Shannon's channel coding theorem,

$$C = \sup_{f_{\mathbf{S}}(\mathbf{S}),\ Tr\{\mathbf{E}(\mathbf{SS^H})\} \le E_s} I(\mathbf{Y}; \mathbf{S}) \quad (6)$$

$$= \sup_{f_{\mathbf{S}}(\mathbf{S}),\ Tr\{\mathbf{E}(\mathbf{SS^H})\} \le E_s} h(\mathbf{Y}) - h(\mathbf{N}) \quad (7)$$

where $Tr\{\mathbf{X}\}$ is the trace of matrix $\mathbf{X}$, $f_{\mathbf{S}}(\mathbf{S})$ is the probability distribution of the transmitted signal and the differential entropy

$$h(\mathbf{X}) = \int_{\mathbf{X}} f_{\mathbf{X}}(\mathbf{x}) \log_2 \left(f_{\mathbf{X}}(\mathbf{x})\right) \mathbf{dx}. \quad (8)$$

The mutual information, $I(\mathbf{Y}; \mathbf{S})$, between the received and transmitted signal on an additive bivariate Middleton Class A noise channel was analyzed under the following conditions.

1) Received signal has Gaussian distribution: An upper bound on mutual information for additive bivariate Middleton Class A noise channel can be evaluated by assuming that the received signal $\mathbf{Y}$ is Gaussian distributed with variance equal to the sum of noise variance and transmitted power. Achieving this upper bound implies that there exists a transmit codebook for every signal-to-noise ratio (SNR), such that the received signal has a Gaussian distribution. This codebook may not exist for all possible SNRs, in which case the channel capacity will be lower than this upper bound.

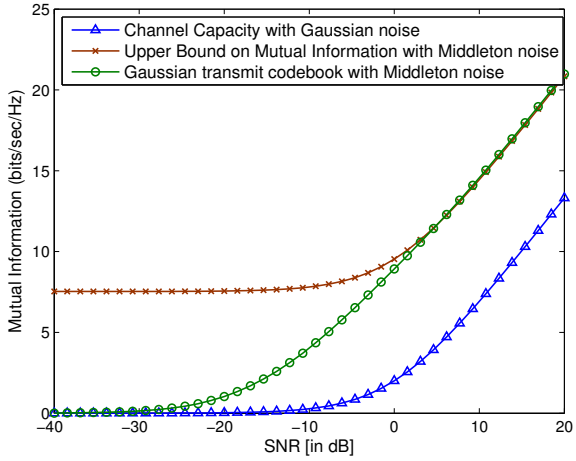

Fig. 1. Mutual information in the presence of Gaussian and bivariate Middleton Class A noise with parameters $A = 0.1$, $\Gamma_1 = 0.01$, $\Gamma_2 = 0.1$ and $\kappa = 0.4$ for a 2×2 MIMO system.

2) Transmitted signal codebook has Gaussian distribution: Mutual information with a Gaussian distributed transmission codebook provides a practical measure of information rate since the transmitted signal are typically Gaussian distributed in communication systems [10]. While this codebook achieves the channel capacity for additive Gaussian noise channels, it is not the optimal codebook to maximize mutual information in the presence of additive bivariate Middleton Class A noise.

The bounds on mutual information for additive bivariate Middleton Class A noise are compared to the capacity of a channel with additive Gaussian noise of equal variance in Fig. 1. The constant gap between the channel capacity in the presence of Middleton Class A noise and the capacity in the presence of Gaussian noise represents the difference between the entropy of Middleton Class A and Gaussian distributions with equal variance. At high SNR, the mutual information under the constraint of Gaussian distributed transmit codebook converges to the upper bound. At low SNR, there may exist a codebook which has higher mutual information than the Gaussian distributed codebook. Deriving such a codebook, however, lies beyond the scope of this paper.

IV. Performance Bounds

A. MAP Decoding Rule

The maximum *a posteriori* (MAP) receiver chooses the codeword which maximizes the *a posteriori* probability $P(\mathbf{S}|\mathbf{Y})$ that codeword $\mathbf{S}$ was sent given that $\mathbf{Y}$ was received. Assuming the channel is memoryless, noise is additive and each codeword is transmitted with equal probability, we can write the MAP decoding rule as

$$\hat{\mathbf{S}} = \arg\max_{\mathbf{S} \in \mathcal{S}} P(\mathbf{S}|\mathbf{Y}) = \arg\max_{\mathbf{S} \in \mathcal{S}} \prod_{t=1}^{T} p(\mathbf{n}_t = \mathbf{y}_t - \mathbf{s}_t) \quad (9)$$

where $\hat{\mathbf{S}}$ is the decoded codeword. Since $\ln(\cdot)$ is a concave function

$$\hat{\mathbf{S}} = \arg\max_{\mathbf{S}\in\mathcal{S}} \omega(\mathbf{S},\mathbf{Y}) = \arg\max_{\mathbf{S}\in\mathcal{S}} \sum_{t=1}^{T} \ln p(\mathbf{n}_t = \mathbf{y}_t - \mathbf{s}_t) \quad (10)$$

where $\omega(\mathbf{S},\mathbf{Y}) = \ln(P(\mathbf{S}|\mathbf{Y}))$. This shows that the MAP detection rule is equivalent to choosing a codeword which maximizes an additive decoding metric $\omega(\mathbf{S},\mathbf{Y})$. This decoding metric assigns a decision region $D(\mathbf{S})$ to each codeword $\mathbf{S}\in\mathcal{S}$, where

$$D(\mathbf{S}) = \{\mathbf{X}|\forall\mathbf{S}'\in\mathcal{S}, \mathbf{S}'\neq\mathbf{S} : \omega(\mathbf{S},\mathbf{X}) > \omega(\mathbf{S}',\mathbf{X})\}. \quad (11)$$

Using the decision region, MAP decoding is equivalent to finding the codeword $\mathbf{S}$ for a given received vector $\mathbf{Y}$, such that $\mathbf{Y}\in\mathcal{D}(\mathbf{S})$. Thus, the probability of a correct decoding decision given that $\mathbf{S}$ was transmitted is given as $P(\mathbf{Y}\in\mathcal{D}(\mathbf{S})|\mathbf{S})$. Correspondingly, the probability of error P_e^{MAP} can be expressed as

$$P_e^{MAP} = 1 - \frac{1}{|\mathcal{S}|}\sum_{\mathbf{S}\in\mathcal{S}} P(\mathbf{Y}\in\mathcal{D}(\mathbf{S})|\mathbf{S}). \quad (12)$$

B. Uncoded Transmission

For uncoded transmission, the MAP decoding metric can be obtained simply by setting the codeword length in (10) to 1. The receiver chooses the symbol $\mathbf{S}$ that minimizes the probability $p(\mathbf{N} = \mathbf{Y} - \mathbf{S})$. The corresponding probability of error can now be calculated as

$$P_e = 1 - \frac{1}{|\mathcal{S}|}\sum_{\mathbf{S}\in\mathcal{S}}\int_{\mathcal{D}(\mathbf{S})} f_{\mathbf{N}}(\mathbf{N} = \mathbf{X} - \mathbf{S})\mathbf{d}\mathbf{X}. \quad (13)$$

For bivariate Class A noise, this error probability was computed through numerically estimating the shape of the decision regions and integrating the noise density function over its corresponding decision region. Fig. 2 shows the probability of error for different values of parameter A. The error probability was also analyzed for uncoded transmission over an additive bivariate Class A channel with a MAP receiver designed for additive Gaussian noise channel. In this scenario, the decision region $\mathcal{D}(\mathbf{s})$ is replaced by a new decision region $\mathcal{D}_g(\mathbf{s})$, that is evaluated assuming that the noise has a Gaussian distribution. The symbol error probability with a Gaussian MAP receiver P_e^G can be expressed as

$$P_e^G = 1 - \frac{1}{|\mathcal{S}|}\sum_{\mathbf{S}\in\mathcal{S}}\int_{\mathcal{D}_g(\mathbf{S})} f_{\mathbf{N}}(\mathbf{N} = \mathbf{X} - \mathbf{S})\mathbf{d}\mathbf{X}. \quad (14)$$

The probability of error for uncoded transmission was evaluated for the additive Class A noise channel with MAP decoding for Class A noise and Gaussian distributed noise. Fig. 2 shows that the probability of error for both types of decoders is very close for the chosen simulation parameters. This is because the decision regions $D(s)$ and $D_g(s)$ are similar in this case. The shape of the symbol error probability curve is also typical for additive Class A noise systems. The distribution function of Class A noise (3) is comprised of two Gaussian components with low and high variance, which are loosely regarded as the thermal noise and impulsive components, respectively. As low SNR, the error probability starts falling since the Gaussian component with low variance is suppressed by increasing SNR. The curve then flattens because the SNR is not sufficiently high to suppress the impulsive component of the Class A noise. The error probability is now limited by the rate of arrival of impulses, which is a fixed quantity and depends solely on parameter A. At high SNR, the curve falls again since both components of Class A noise are being suppressed. This particular nature of error probability also occurs during analysis of receiver design in Middleton noise in [2], [6] and [8].

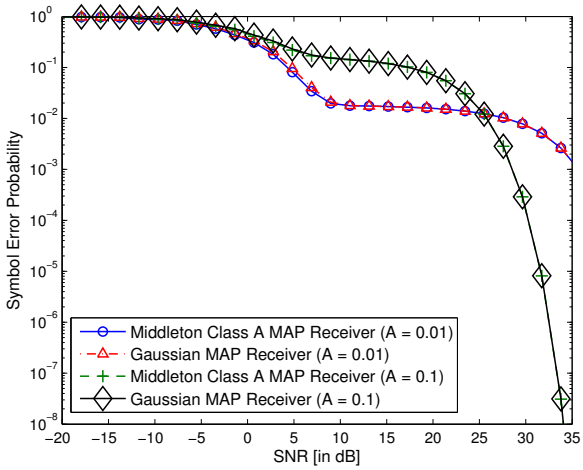

Fig. 2. Symbol error probability with MAP decoding rule for Gaussian and Middleton Class A noise under additive bivariate Middleton Class A noise with parameters $\Gamma_1 = 0.01$, $\Gamma_2 = 0.1$ and $\kappa = 0.4$. The error probability curves for Gaussian and Middleton Class A noise MAP receivers are indistinguishably close in this figure.

C. Coded Transmission

In the case of coded transmission, the union bound on the error probability can be used to obtain a asymptotically tight upper bound given as

$$P_e \leq \frac{1}{|\mathcal{S}|}\sum_{\mathbf{S}\in\mathcal{S}}\sum_{\mathbf{S}'\in\mathcal{S},\mathbf{S}'\neq\mathbf{S}} P(\mathbf{S}\to\mathbf{S}') \quad (15)$$

where $P(\mathbf{S}\to\mathbf{S}')$ is the pairwise error probability (PEP). The PEP represents a decoding error in a binary decision between the codewords $\mathbf{S}'$ and $\mathbf{S}$ and can be expressed as

$$P(\mathbf{S}\to\mathbf{S}') = P\left(w(\mathbf{S}',\mathbf{Y}) - w(\mathbf{S},\mathbf{Y}) > 0 \mid \mathbf{S}\right). \quad (16)$$

Using Chernoff bounding techniques [4], the PEP has an upper bound as follows

$$P(\mathbf{S}\to\mathbf{S}') \leq \min_{\lambda}\prod_{t=1}^{T} C(\mathbf{s}_t,\mathbf{s}_t',\lambda) \quad (17)$$

where the Chernoff factors

$$C(\mathbf{s}_t,\mathbf{s}_t',\lambda) = \int_{-\infty}^{\infty} e^{\lambda\left(w(\mathbf{s}_t',\mathbf{y}_t)-w(\mathbf{s}_t,\mathbf{y}_t)\right)} f\left(\mathbf{n}_t = \mathbf{y}_t - \mathbf{s}_t\right) d\mathbf{y}_t. \quad (18)$$

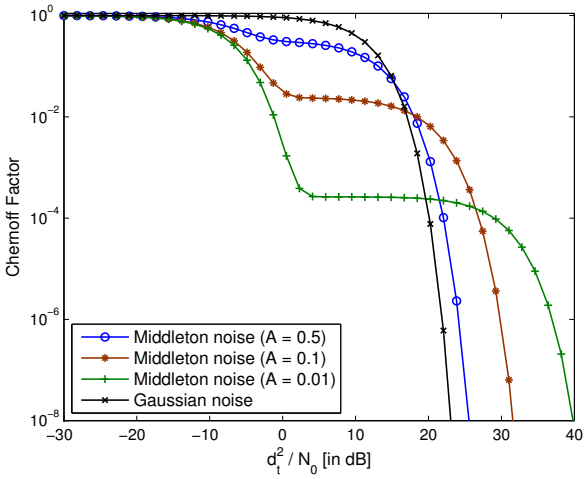

Fig. 3. Chernoff Factors with MAP decoding MIMO receiver in presence of Gaussian and bivariate Middleton Class A noise with parameters $\Gamma_1 = 0.01$, $\Gamma_2 = 0.1$ and $\kappa = 0.4$.

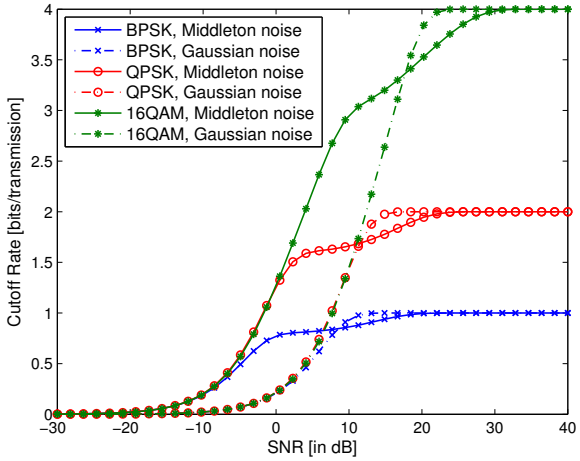

Fig. 4. Cutoff Rate with MAP decoding MIMO receiver in presence of Gaussian and bivariate Middleton Class A noise with parameters $A = 0.1$, $\Gamma_1 = 0.01$, $\Gamma_2 = 0.1$ and $\kappa = 0.4$.

In (18), the integration is four-dimensional for a complex channel with two receive antennas. If MAP decoding is used, $\lambda = 1/2$ minimizes the Chernoff factors [4] and tightens the bound in (17). Since a binary decision between the codewords $\mathbf{s}$ and $\mathbf{s}'$ is considered, the Chernoff factors are a function of the distance, $\mathbf{d}_t = \mathbf{s}_t - \mathbf{s}'_t$, between the codewords. For *i.i.d.* in-phase and quadrature phase noise components, this yields

$$C^{MAP}(\mathbf{d}_t) = \int_{-\infty}^{\infty} \sqrt{f_{\mathbf{n}_I}\left(\mathbf{n}'_{t,I}\right) f_{\mathbf{n}_I}\left(\mathbf{n}_{t,I}\right)} d\mathbf{y}_{t,I} \times \int_{-\infty}^{\infty} \sqrt{f_{\mathbf{n}_Q}\left(\mathbf{n}'_{t,Q}\right) f_{\mathbf{n}_Q}\left(\mathbf{n}_{t,Q}\right)} d\mathbf{y}_{t,Q} \quad (19)$$

where $\mathbf{n}_t = \mathbf{y}_t - \mathbf{s}_t$ and $\mathbf{n}'_t = \mathbf{y}_t - \mathbf{s}'_t$ and each integration is two-dimensional for two a receive antenna system.

To quantify the throughput performance of coded transmission, we derive the cutoff rate R_0 based on random coding arguments. Cutoff rate provides a similar metric to the channel capacity and relates the transmission rate R, expressed as the average number of information bits per channel use, to the decoding error probability for a length T code as

$$P_e < e^{-T(R_0 - R)}. \quad (20)$$

Hence it shows that for any transmission rate $R < R_0$, an arbitrarily small error probability can be achieved by increasing the code length T. Assuming every code symbol in $\mathcal{X}$ is equally likely to be transmitted and MAP decoding is performed at the receiver, the cutoff rate can be expressed using the Chernoff factors as

$$R_0 = -\log_2 \frac{1}{|\mathcal{X}|^2} \sum_{\mathbf{s}\in\mathcal{X}} \sum_{\mathbf{s}'\in\mathcal{X}} C^{MAP}(\mathbf{d} = \mathbf{s} - \mathbf{s}'). \quad (21)$$

Fig. 3 compares the Chernoff factors for MAP decoding in the presence of additive bivariate Middleton Class A noise. Chernoff factors in the presence of Gaussian noise is also plotted.

Fig. 4 compares the cutoff rate in the presence of bivariate Middleton Class A noise with the cutoff rate in the presence of Gaussian noise for coded transmissions using BPSK, QPSK and 16QAM modulation and spatial multiplexing mode of transmission. The plateau in the curves at moderately high SNR in the Chernoff bounds and cutoff rate is consistent with the explanation provided in Sec. IV-B for probability of symbol error in uncoded transmissions.

REFERENCES

[1] M. Nassar, K. Gulati, A. K. Sujeeth, N. Aghasadeghi, B. L. Evans, and K. R. Tinsley, "Mitigating near-field interference in laptop embedded wireless transceivers," in *Proc. IEEE Int. Conf. on Acoustics, Speech, and Signal Proc.*, Mar. 30-Apr. 4 2008.

[2] A. Li, Y. Wang, W. Xu, and Z. Zhou, "Performance evaluation of MIMO systems in a mixture of Gaussian noise and impulsive noise," in *Proc. IEEE Joint Conf. Asia-Pacific Conf. on Comm. and Int. Symp. Multi-Dim. Mobile Comm.*, vol. 1, Aug. 29-Sept. 1 2004, pp. 292–296.

[3] D. Middleton, "Non-Gaussian noise models in signal processing for telecommunications: New methods and results for Class A and Class B noise models," *IEEE Trans. on Info. Theory*, vol. 45, no. 4, pp. 1129 – 1149, May 1999.

[4] J. Haring and A. J. H. Vinck, "Performance bounds for optimum and suboptimum reception under Class-A impulsive noise," *IEEE Trans. for Comm.*, vol. 50, no. 7, pp. 1130– 1136, 2002.

[5] R. Blum, R. Kozick, and B. Sadler, "An adaptive spatial diversity receiver for non-Gaussian interference and noise," in *Proc. IEEE Int. Work. Signal Proc. Adv. in Wireless Comm.*, April 1997, pp. 385–388.

[6] P. A. Delaney, "Signal detection in multivariate Class-A interference," *IEEE Trans. on Comm.*, vol. 43, no. 4, pp. 365–373, April 1995.

[7] K. F. McDonald and R. S. Blum, "A statistical and physical mechanisms-based interference and noise model for array observations," *IEEE Trans. on Signal Proc.*, vol. 48, pp. 2044 – 2056, July 2000.

[8] K. Gulati, A. Chopra, R. W. Heath, B. L. Evans, K. R. Tinsley, and X. E. Lin, "MIMO receiver design in the presence of radio frequency interference," in *Proc. IEEE Global Comm. Conf.*, Dec 2008.

[9] S. M. Zabin and H. V. Poor, "Efficient estimation of Class A noise parameters via the EM algorithms," *IEEE Trans. on Info. Theory*, vol. 37, no. 1, pp. 60–72, Jan 1991.

[10] T. M. Cover and J. A. Thomas, *Elements of Information Theory*, 2nd ed. Wiley & Sons, New York, 2006.